Quantum coherence controls the charge separation in a prototypical artificial light harvesting system

Carlo Andrea Rozzi[1†], Sarah Maria Falke[2†], Nicola Spallanzani[1,3], Angel Rubio[4,5], Elisa Molinari[1,3*], Daniele Brida[6], Margherita Maiuri[6], Giulio Cerullo[6], Heiko Schramm[7], Jens Christoffers[7] & Christoph Lienau[2*]

1. Istituto Nanoscienze – CNR, Centro S3, via Campi 213a, I-41125 Modena, Italy
2. Institut für Physik and Center of Interface Science, Carl von Ossietzky Universität, 26111 Oldenburg, Germany.
3. Dipartimento di Fisica, Università di Modena e Reggio Emilia. via Campi 213a I-41125 Modena, Italy
4. Nano-Bio Spectroscopy Group and ETSF Scientific Development Centre, Dpto. Física de Materiales, Universidad del País Vasco, Centro de Física de Materiales CSIC-UPV/EHU-MPC and DIPC, Av. Tolosa 72, E-20018 San Sebastián, Spain
5. Fritz-Haber-Institut der Max-Planck-Gesellschaft, Berlin, Germany
6. IFN-CNR, Dipartimento di Fisica, Politecnico di Milano, Milano, Italy
7. Institut für Reine und Angewandte Chemie and Center of Interface Science, Carl von Ossietzky Universität, 26111 Oldenburg, Germany.

[†]Both authors contributed equally to this work
[*]Authors to whom correspondence should be addressed

The efficient conversion of light into electricity or chemical fuels is a fundamental challenge. In artificial photosynthetic and photovoltaic devices this conversion is generally thought to happen on ultrafast, femto-to-picosecond time scales and to involve an incoherent electron transfer process. In some biological systems, however, there is growing evidence that the coherent motion of electronic wavepackets is an essential primary step, raising questions about the role of quantum coherence in artificial devices. Here we investigate the primary charge transfer process in a supramolecular triad, a prototypical artificial reaction center. Combining high time-resolution femtosecond spectroscopy and time-dependent density functional theory, we provide compelling evidence that the driving mechanism of the photoinduced current generation cycle is a correlated wavelike motion of electrons and nuclei on a timescale of few tens of femtoseconds. We highlight the fundamental role of the interface between chromophore and charge acceptor in triggering the coherent wavelike electron-hole splitting.

(150 Words)

Introduction

Nature has developed sophisticated and highly efficient molecular architectures to convert sunlight into chemical energy, which is then used to nurture plants. On a microscopic level, photosynthesis consists of the following processes: light harvesting via a cascade of energy transfer steps, subsequent charge separation at the reaction center and multi-electron catalysis. One of the key challenges for the future will be to learn how to construct artificial molecular devices enabling the harvesting of sunlight and their use either for direct electric power generation (photovoltaic approach)[1-3] or to drive fuel-producing photochemical reactions (photosynthetic approach)[4,5]. Very recently, the observation of electronic quantum coherence, i.e. the wavelike motion of electrons, induced a paradigm shift[6] in describing the primary energy and charge transfer processes both in photosynthetic bacteria[7] and in higher plants[8-10]. A fascinating, but so far unexplored, perspective would be to exploit such quantum coherence effects in artificial photosynthetic/photovoltaic systems in order to excel their performance.

Here we study the dynamics of a photoexcited supramolecular carotene-porphyrin-fullerene triad[11,12], which is a prototypical artificial reaction center, by means of high time-resolution femtosecond spectroscopy and first-principles quantum-dynamical simulations. Upon photoexcitation of the porphyrin moiety, the primary event is the electron transfer to the fullerene[13]. We provide compelling evidence that the driving mechanism of this process is a correlated wavelike motion of electrons and nuclei on a timescale of few tens of femtoseconds, thus establishing the role of vibronic coherence in artificial light harvesting.

Results

We chose a supramolecular carotene-porphyrin-fullerene triad, rather than the conceptually simpler porphyrin/fullerene dyad, as a model for exploring charge transfer dynamics[14,15] because of the protective role of the carotene, suppressing photobleaching. The compound consists of a porphyrin ring acting as the primary light absorber, a fullerene electron acceptor and a carotene group serving as a hole stabilizer (Fig. 1a). It is known that photoexcitation of the porphyrin triggers an ultrafast electron transfer to the fullerene[13] with a charge separation yield of up to 95%[11]. Subsequent electron transfer from the carotene to the porphyrin cation on a 100 ps time scale forms a long-lived charge-separated state which decays back to the ground state via the radical-pair mechanism on a microsecond timescale. The optical properties of this and similar triads were carefully investigated experimentally[12], but the microscopic mechanisms underlying the charge transfer dynamics on a femtosecond timescale could not be unveiled due to insufficient time resolution.

Steady-state optical absorption spectra of the triad in toluene solution (Fig. 1b) show the characteristic peaks of the Soret- and the Q-band of the porphyrin moiety[16]. The broad absorption of the carotene group sets in at around 550 nm and peaks at ≈510 nm. The fullerene unit induces a continuous weak absorption background throughout the visible. The assignment of these spectra is facilitated by comparison with subunit spectra of a porphyrin-fullerene dyad and of the porphyrin unit (Fig. 1b), and provides no evidence of charge-transfer excitations. We have calculated the absorption spectra of the triad and its subunits (Fig. 1c) using first-principles simulations within time-dependent density functional theory (TDDFT)[17-19] in Local Density Approximation. The strong Soret band and

some features of the weaker Q-band of the porphyrin are well reproduced when red-shifting the theoretical wavelength axis by 180 meV. The dominant carotene absorption band appears red-shifted to 730 nm and is better attributed to the carotene radical cation, due to the neglect of double excitations and strong excitonic correlations[20,21] at this level of TDDFT.

To probe the electron-hole splitting dynamics we used a 7-fs pulse centered around 550 nm to impulsively excite the Q-band of the porphyrin group in the triad (see Fig. S3 of the Supplementary information). Due to its broad bandwidth this excitation pulse also couples to the S_2 state of the carotene moiety and this leads to an excited state absorption from the optically dark S_1 state of carotene after a 200-fs internal conversion process between these states[22-24]. Most notably, the impulsive excitation induces a large amplitude vibrational motion in the ground electronic state of the carotene moiety leading to pronounced oscillatory modulation of the $\Delta T/T$ spectra. To gain insight into the charge-transfer dynamics in the triad, we have analyzed these known oscillations[24] using well-established density matrix formalism[25] and subtracted them from the original data to obtain the $\Delta T/T$ spectra shown in Fig. 2a. These time-dependent spectra show two prominent features, (i) a long-lived photobleaching of the porphyrin Q-band absorption resonance around 523 nm and (ii) a short-lived and spectrally red-shifting transient emission band in the region between 540 nm and 580 nm. The long-lived oscillatory modulation on the Q-band resonance at later times tracks impulsively excited vibrational motion in the ground state of the porphyrin moiety.

A striking and novel signature of these measurements is the transient increase in

transmission in the 540-580 nm region. Due to its pronounced spectral shift with time we cannot assign it to one of the known ground state optical transitions of the individual subunits of the triad and hence we attribute it to a stimulated emission (SE) from the photoexcited electronic state. We can only track this SE for a time period of about 100 fs which means that this emission is not coming from the final charge separated state but rather from a transient intermediate. The data in Fig. 2 suggest temporal oscillations of not only the amplitude (Fig. 2b) but also the resonance wavelength (Fig. 2c) of this band with a period of about 30 fs. The oscillations in the resonance wavelength are not compatible with a simplified picture in which the excited electronic wavepacket moves ballistically from the donor to the acceptor state[26]. We interpret them as signature of coherent charge oscillations between donor and acceptor state.

We performed a detailed TDDFT quantum-dynamical description of the system in order to clarify the influence of coherent charge motion on the electron transfer dynamics. Since no direct charge-transfer excitations are involved in the photoexcitation, the simple local approximation is expected to well describe the electron-ion dynamics during the initial charge separation. For instance, even though the energy of the final state is likely underestimated by the approximations of the model, other important features such as the low frequency response of the charge density resulted to be robust against the final state[27]. We have modeled the initial photoexcitation of the molecule as a sudden change in the charge density localized on the porphyrin moiety, and the resulting motion of charges and ions was tracked in space and time. In this way, we ensure that no charge is displaced to the fullerene at time zero and that we realistically mimic the Franck-Condon excitation of the porphyrine moiety occurring in the experiment. The quantum dynamics simulations suggest

a rapid and almost complete charge flow to the fullerene moiety within about 70 fs (Figs. 3a and 3b). On this time scale, the launched electronic wavepacket oscillates a few times, with a period of 30 fs, back and forth between the carotene-porphyrin group and the fullerene moiety. Both the time scale of the charge build-up and the oscillation period of the electronic wavepacket agree well with the experimentally observed values (Fig. 3b). The agreement becomes even more striking by comparing Fourier spectra of the simulated charge transfer dynamics (Fig. 4a) to those of the experimental amplitude and resonance wavelength dynamics (Fig. 4b). For both the experimental amplitude data and the simulated charge dynamics the spectra reveal a distinct peak at about 1000 cm^{-1}, corresponding to an oscillation period of 33 fs. Even the Fourier transform of the strongly red-shifting resonance wavelength (inset in Fig. 4b) reveals a dominant resonance at 930 cm^{-1} (36 fs), although the weak oscillatory contrast on the time-resolved data in Fig. 2 precludes a quantitative assignment of the spectrum. Within the accuracy of the presented results, the experimentally observed and simulated oscillation period of about 30 fs is reasonably close to that of the carbon backbone vibrations, with a frequency of the dominant excited-state C-C stretch motion of 1230 cm^{-1} [28]. This suggests that nuclear motion delocalized across the porphyrin/fullerene region drives the charge transfer. This conclusion is strongly supported by the small change in the transfer dynamics observed in the simulations when the positions of either the carotene or the fullerene ions are blocked (Fig. 3a). On the other hand, even minor changes of the nuclear vibrations in the porphyrin/linker region of the molecule can greatly influence the charge flow. Upon locking the porphyrin ions or only 4 atoms on the aryl-ring connecting porphyrin and fullerene, charge accumulation on the fullerene is greatly suppressed (Fig. 3a) while the coherent charge oscillations at the backbone

vibrational frequency still persist. Fixing the position of all ions, on the other hand, suppresses both charge oscillation and accumulation. Several movies in the Supplementary information summarize the results of the simulations (Movie S1-S3). In general, we find that the TDDFT calculations provide an estimate of the overall time scale of the charge transfer process of about 70 fs which is in quite good agreement with that deduced from the shift in resonance wavelength of the charge transfer band seen in Fig. 2b. Also the period of the predicted charge oscillations of about 30 fs agrees well with our experimental measurements. Remaining differences in the phase of those oscillatory patterns (Fig. 3b) likely reflect the different excitation and probing conditions in experiment and theory and possible small uncertainties (a few fs) in the measurement of the experimental time zero. Both experimental and theoretical results suggest that the charge degrees of freedom in our molecule are strongly coupled to the carbon backbone vibration. A detailed understanding of this coupling mechanism requires a refined analysis of the potential energy surfaces of this large molecule, specifically of conformational changes between ground and excited electronic states. Such information is beyond the scope of the mean field Ehrenfest approach presented here. A deeper quantum-chemical analysis of the coupling mechanism is currently underway.

Our results shed new light onto the microscopic origin of the experimentally observed charge transfer dynamics. Clearly, a simplified, often assumed static picture of molecular level alignment[29,30] is not sufficient to describe the first steps of the charge separation process[14,15]. Instead a coherent dynamical picture emerges as the correct physical framework for the splitting of the photogenerated electron-hole pair. Optical excitation launches an electronic wave packet onto the excited state surface of the absorber. This

simultaneously induces coherent nuclear motion of the carbon backbone and charge oscillations between the absorber and the acceptor. The transient charge generation on the acceptor leads to a gradual rearrangement of the molecular geometry and a concomitant time-dependent change of the acceptor potential energy surface. This dynamical geometric rearrangement is necessary to stabilize the charge accumulation on the acceptor and gives rise to the experimentally observed red shift of the SE spectrum. Hence, it is the concerted coherent motion of strongly coupled electrons and ions that drives the charge separation in this triad, while the surrounding environment, specifically the polarity of the solvent, apparently plays a less important role, in accordance with previous observations[11].

Taken together, our experimental and theoretical data provide compelling evidence that the correlated, quantum-coherent motion of ions and electrons not only governs the first steps of the photo-induced electron dynamics but also the yield of the charge separation in this prototypical artificial light-harvesting system, in stark contrast to prevailing statistical models for electron transfer reactions. Specifically our results suggest that the carbon backbone motion promotes coherent charge oscillations while rapid geometric rearrangements of the donor-acceptor structure are crucial in stabilizing the separated charges. This implies that not only the geometric and electronic structure of a photovoltaic material, but also the flexibility of its molecular structure, and in particular of the donor and donor-acceptor linking group, is an important parameter for optimizing its yield. It seems interesting to explore this new optimization parameter and to further test interface quantum coherence effects in technologically relevant devices in order to improve their performance.

Methods

Chemical synthesis:

For the synthesis of the triad the three different modules, i. e. the porphyrin-, the fullerene- and the carotenoid-part were prepared separately and finally linked together by a 1,3-dipolar cycloaddition and amide formation according to a literature protocol[11]. The formation of the porphyrin-part started from pyrrole and mesitylaldehyde. The resulting dipyrromethane was condensed with methyl 4-formylbenzoate to form the symmetric 5,15-dimesityl-10,20-bis[4-(methoxycarbonyl)phenyl]porphyrin by a known procedure[31-33].

Several functional group interconversions[34] led to a porphyrin with a carboxylic acid at the western end (cf. Fig. 1a), which is needed for the already mentioned final amidation step. A carbaldehyde group was implemented at the eastern end, which was converted with fullerene in a 1,3-dipolar cycloaddition of an azomethine ylide (prepared from *N*-methylglycine in situ) to form the porphyrin-fullerene-module of the triad[35].

The carotenoid-part of the triad had been prepared before, but the established synthesis[36] turned out to give unsatisfactory results. Therefore, a new two-step synthesis was developed, starting from 4-nitrobenzyltriphenylphosphoniumbromide which was reduced to the aniline in the first step with H_2 and Pd/C[37]. The second step was a Wittig-reaction with apocarotinal to form the desired carotenoid.

Experimental

The femtosecond transient absorption spectrometer starts with a regeneratively-amplified

mode-locked Ti:Sapphire laser system (Clark-MXR model CPA-1) delivering pulses with 150-fs duration, 500-μJ energy, at 1-kHz repetition rate and 780-nm central wavelength. The system drives three independent non-collinear optical parametric amplifiers (NOPAs)[38], which generate the pump and the probe pulses for the time-resolved experiments. The first NOPA (NOPA1) generates broadband visible pump pulses at 550-nm, compressed to 10-fs duration by multiple bounces on custom-designed chirped mirrors; these pulses are used to resonantly excite the Q-band of the porphyrin. The second NOPA (NOPA2) generates broadband pulses in the near-infrared frequency range (from 820 nm to 1020 nm), which are compressed by a Brewster-cut fused-silica prism pair and up-converted to 420 nm by sum-frequency generation with the 780-nm laser pulses, resulting in a 15-fs pulsewidth. Pulses from NOPA2 are used to resonantly excite the Soret band of the porphyrin. The third NOPA (NOPA3) generates broadband visible pulses (500-700 nm range) compressed to 7-fs duration by a pair of chirped mirrors and used to probe the transient absorption of the triad. Supplementary Fig. S1 shows typical spectra from the three NOPAs.

The sample is contained in a cuvette with 250-μm-thick fused-silica windows and ~300-μm optical path. After the sample, the probe beam is selected by an iris and focused onto the entrance slit of a spectrometer equipped with a 1024-pixel linear photodiode array and electronics specially designed for fast read-out times and low noise[39]. The spectral resolution of the spectrograph (about 2 nm) is largely sufficient for our experiments. A fast analog-to-digital conversion card with 16-bits resolution enables single-shot recording of the probe spectrum at the full 1-kHz repetition rate. By recording pump-on and pump-off

probe spectra, one can calculate the differential transmission ($\Delta T / T$) spectrum at the specific probe delay τ as:

By repeating this procedure for a few hundred milliseconds and averaging the resulting signals, it is thus possible to achieve a high enough signal to noise ratio. By moving the translation stage we record $\Delta T / T$ spectra at different probe delays, thus obtaining a complete 2D map:  .

Theoretical

TDDFT simulations of the coupled electron and ion dynamics of the triad were carried out in gas phase on a molecule without porphyrin side groups at the Local Density Approximation (LDA) level using the Perdew-Zunger correlation functional with the open source code `octopus`[17]. The system was described on a real space grid with a 0.2 Å spacing and propagated in time for 72.8 fs in total, with a time step of 1.7 as. The time propagator was approximated by a fourth order Taylor expansion[17]. The core electrons were represented via Troullier-Martins pseudopotentials (for *s*, *p*, and *d* components, the cutoff radii of the pseudo-potentials are 1.25 bohr for Hydrogen atoms, 1.47 bohr for carbon atoms, and 1.39 bohr for Nitrogen and Oxygen atoms), and the interpolating scaling functions method[40] was used to efficiently solve the Poisson equation in the calculation of the Hartree potential. Time-dependent optical spectra were calculated by propagating the state of the system for additional 18.6 fs after the charge density underwent an impulsive perturbation at given times. The orbitals were propagated with the time-symmetry enforced

method[41] using a Lanczos algorithm to evaluate the propagation operator with a time step of 7.9 as, resulting in a spectral range window for the dynamical polarizability of at least 8 eV. In all present calculations the nuclei are considered as classical particles, but the ion-electron dynamics is treated with an Ehrenfest scheme controlled at the electronic propagation time-step[42,43]. This approximation is expected to adequately describe the electron-ion dynamics during the initial charge separation process even though the energetics of the final state are evidently affected by the approximations introduced at this level of DFT.

References

1. Scholes, G. D., Fleming, G. R., Olaya-Castro, A. & van Grondelle, R. Lessons from nature about solar light harvesting. *Nature Chem.* **3,** 763-774 (2011).

2. Blankenship, R. E. *et al.* Comparing Photosynthetic and Photovoltaic Efficiencies and Recognizing the Potential for Improvement. *Science* **332,** 805-809 (2011).

3. Gratzel, M. Photoelectrochemical cells. *Nature* **414,** 338-344 (2001).

4. Brabec, C. J., Sariciftci, N. S. & Hummelen, J. C. Plastic solar cells. *Adv. Funct. Mater.* **11,** 15-26 (2001).

5. Huynh, W. U., Dittmer, J. J. & Alivisatos, A. P. Hybrid nanorod-polymer solar cells. *Science* **295,** 2425-2427 (2002).

6. Engel, G. S. *et al.* Evidence for wavelike energy transfer through quantum coherence in photosynthetic systems. *Nature* **446,** 782-786 (2007).

7. Collini, E. *et al.* Coherently wired light-harvesting in photosynthetic marine algae at ambient temperature. *Nature* **463,** 644-647 (2010).

8. Ishizaki, A. & Fleming, G. R. Theoretical examination of quantum coherence in a photosynthetic system at physiological temperature. *Proc. Natl. Acad. Sci. USA* **106,** 17255-17260 (2009).

9. Abramavicius, D. & Mukamel, S. Energy-transfer and charge-separation pathways in the reaction center of photosystem II revealed by coherent two-dimensional optical spectroscopy. *J. Chem. Phys*. **133,** 184501 (2010).

10. Lee, H., Cheng, Y.-C. & Fleming, G. R. Coherence dynamics in photosynthesis: Protein protection of excitonic coherence. *Science* **316,** 1462-1465 (2007).

11. Kodis, G., Liddell, P. A., Moore, A. L., Moore, T. A. & Gust, D. Synthesis and photochemistry of a carotene-porphyrin-fullerene model photosynthetic reaction center. *J. Phys. Org. Chem.* **17,** 724-734 (2004).

12. Gust, D., Moore, T. A. & Moore, A. L. Mimicking photosynthetic solar energy transduction. *Acc. Chem. Res.* **34,** 40-48 (2001).

13. Kuciauskas, D. *et* a*l.* Photoinduced electron transfer in carotenoporphyrin-fullerene triads: Temperature and solvent effects. *J.* P*hys. Chem. B* **104,** 4307-4321 (2000).

14. Brabec, C. J. *et al.* Tracing photoinduced electron transfer process in conjugated polymer/fullerene bulk heterojunctions in real time. *Chem. Phys. Lett.* **340,** 232-236 (2001).

15. Huber, R., Moser, J. E., Gratzel, M. & Wachtveitl, J. Real-time observation of photoinduced adiabatic electron transfer in strongly coupled dye/semiconductor colloidal systems with a 6 fs time constant. *J. Phys. Chem. B* **106,** 6494-6499 (2002).

16. Baskin, J. S., Yu, H. Z. & Zewail, A. H. Ultrafast dynamics of Porphyrins in the condensed phase: I. Free base tetraphenylporphyrin. *J. Phys. Chem. A* **106,** 9837-9844 (2002).

17. Castro, A. *et al.* Octopus: a tool for the application of time-dependent density functional theory. *Phys. Status Solidi* B **243,** 2465-2488 (2006).

18. Baruah, T. & Pederson, M. R. DFT Calculations on Charge-Transfer States of a Carotenoid-Porphyrin-C(60) Molecular Triad. *J. Chem. Theory Comput.* **5,** 834-843 (2009).

19. Spallanzani, N. *et al.* Photoexcitation of a Light-Harvesting Supramolecular Triad: A Time-Dependent DFT Study. *J. Phys. Chem. B* **113,** 5345-5349 (2009).

20. Starcke, J. H., Wormit, M., Schirmer, J. & Dreuw, A. How much double excitation character do the lowest excited states of linear polyenes have? *Chem. Phys.* **329,** 39-49 (2006).

21. Varsano, D., Marini, A. & Rubio, A. Optical saturation driven by exciton confinement in molecular chains: A time-dependent density-functional theory approach. *Phys. Rev. Lett.* **101,** 133002 (2008).

22. Cerullo, G. *et al.* Photosynthetic light harvesting by carotenoids: Detection of an intermediate excited state. *Science* **298,** 2395-2398 (2002).

23. Wohlleben, W. *et al.* Pump-deplete-probe spectroscopy and the puzzle of carotenoid dark states. *J. Phys. Chem. B* **108,** 3320-3325 (2004).

24. Polli, D. *et al.* Broadband pump-probe spectroscopy with sub-10-fs resolution for probing ultrafast internal conversion and coherent phonons in carotenoids. *Chem. Phys.* **350,** 45-55 (2008).

25. Kumar, A. T. N., Rosca, F., Widom, A. & Champion, P. M. Investigations of amplitude and phase excitation profiles in femtosecond coherence spectroscopy. *J. Chem. Phys.* **114,** 701-724 (2001).

26. Polli, D. *et al.* Conical intersection dynamics of the primary photoisomerization event in vision. *Nature* **467,** 440-443 (2010).

27. Marques, M. A. L, Ullrich, C. A., Nogueira, F., Rubio, A., Burke, K. & Gross, E. K. U. (Editors), *Time-Dependent Density Functional Theory, Lecture Notes in Physics* vol. 620, (Springer, 2003).

28. Hornung, T., Skenderovich, H. & Motzkus, M. Observation of all-trans-beta-carotene wavepacket motion on the electronic ground and excited dark state using degenerate four-wave mixing (DFWM) and pump-DFWM., *Chem. Phys. Lett.* **402,** 283-288 (2005).

29. Marcus, R. A. Electron-transfer reactions in chemistry – theory and experiment. *Rev. Mod. Phys.* **65,** 599-610 (1993).

30. Duncan, W. R. & Prezhdo, O. V. Theoretical studies of photoinduced electron transfer in dye-sensitized TiO(2). *Annu. Rev. Phys. Chem.* **58,** 143-184 (2007).

31. Lee, C. H. & Lindsey, J. S. One-Flask Synthesis of Meso-Substituted Dipyromethanes and Their Application in the Synthesis of *Trans*-Substituted Porphyrin Building Blocks. *Tetrahedron* **50,** 11427-11440 (1994).

32. Boyle, R. W., Bruckner, C., Posakony, J., James, B. R. & Dolphin, D. 5-Phenyldipyrromethane and 5,15-diphenylporphyrin. *Org. Synth.* **76,** 287-293 (1999).

33. Carcel, C. M. *et al.* Porphyrin Architectures Tailored for Studies of Molecular Information Storage. *J. Org. Chem.* **69,** 6739-6750 (2004).

34. Liddell, P. A. *et al.* Photoinduced Electron Transfer in Tetrathiafulvalene-Porphyrin-Fullerene Molecular Triads. *Helv. Chim. Acta* **84,** 2765-2783 (2001).

35. Tagmatarchis, N. & Prato, M. The addition of Azomethine Ylides to [60]Fullerene Leading to Fulleropyrrolidines. *Synlett* **6,** 768-779 (2003).

36. Gust, D. *et al.* Triplet and Singlet Energy Transfer in Carotene Porphyrin Dyads: Role of the Linkage Bonds. *J. Am. Chem. Soc.* **114**, 3590-3603 (1992).

37. Horner, L., Hoffmann, H., Wippel, H. G. & Hassel, G. Zum Spaltungsverlauf gemischt substituierter Tetraaryl-phosphonium-hydroxide. *Chem. Ber.* **91,** 52-57 (1958).

38. Manzoni, C., Polli, D. & Cerullo, G. Two-color pump-probe system broadly tunable

over the visible and the near infrared with sub-30 fs temporal resolution. *Rev. Sci. Instrum.* **77,** 023103 (2006).

39. Polli, D., Lüer, L. & Cerullo, G. High-time-resolution pump-probe system with broadband detection for the study of time-domain vibrational dynamics. *Rev. Sci. Instrum.* **78,** 103108 (2007).

40. Genovese, L., Deutsch, T., Neelov, A., Goedecker, S. & Beylkin, G. Efficient solution of Poisson's equation with free boundary conditions. *J. Chem. Phys.* **125,** 074105 (2006).

41. Castro, A., Marques, M. A. L. & Rubio, A. Propagators for the time-dependent Kohn-Sham equations. *J. Chem. Phys.* **121,** 3425-3433 (2004).

42. Alonso, J. *et al.* Efficient formalism for large-scale ab initio molecular dynamics based on time-dependent density functional theory. *Phys. Rev. Lett.* **101,** 096403 (2008).

43. Andrade, X. *et al.* Modified Ehrenfest Formalism for Efficient Large-Scale ab initio Molecular Dynamics. *J. Chem. Theory Comput.* **5**, 728-742 (2009).

Acknowledgments

The computer resources for the simulations were provided by CINECA, Italy, ISCRA project n. HP10BWZPJA. The work in Germany was funded by the Deutsche Forschungsgemeinschaft (SPP1391 and DFG-NSF Materials World Network) and by the Korea Foundation for International Cooperation of Science and Technology (Global

Research Laboratory Project K20815000003). SMF is grateful for a PhD fellowship from "Stiftung der Metallindustrie im Nord-Westen". AR acknowledges financial support from the European Research Council Advanced Grant DYNamo (ERC-2010-AdG No. 267374), Spanish MICINN (FIS2010-65702-C02-01, PIB2010US-00652 and /CSD2010-00044/), ACI-Promociona (ACI2009-1036) and Grupos Consolidados UPV/EHU del Gobierno Vasco (IT-319-07). GC acknowledges financial support from the PRIN programme 2008JKBBK4.

Author Contributions

C.A.R., E.M., S.M.F., G.C., A.R. and C. L. initiated this work. H.S. and J.C. synthesized the molecule. D.B., M.M. and S.M.F. conducted the experiments. C.A.R., N.S., A.R. and E.M. contributed to the theoretical study of the triad. C.A.R. and N.S. performed the TDDFT simulations. All authors discussed the results and implications at all stages. C.A.R., S.M.F. and C.L. designed the paper. All authors contributed to the writing of the paper.

Author Information

C.A.R. and S.M.F. contributed equally to this work. The authors declare no competing financial interest. Correspondence and requests for materials should be addressed to E.M. (elisa.molinari@unimore.it) or C.L. (christoph.lienau@uni-oldenburg.de).

Figures

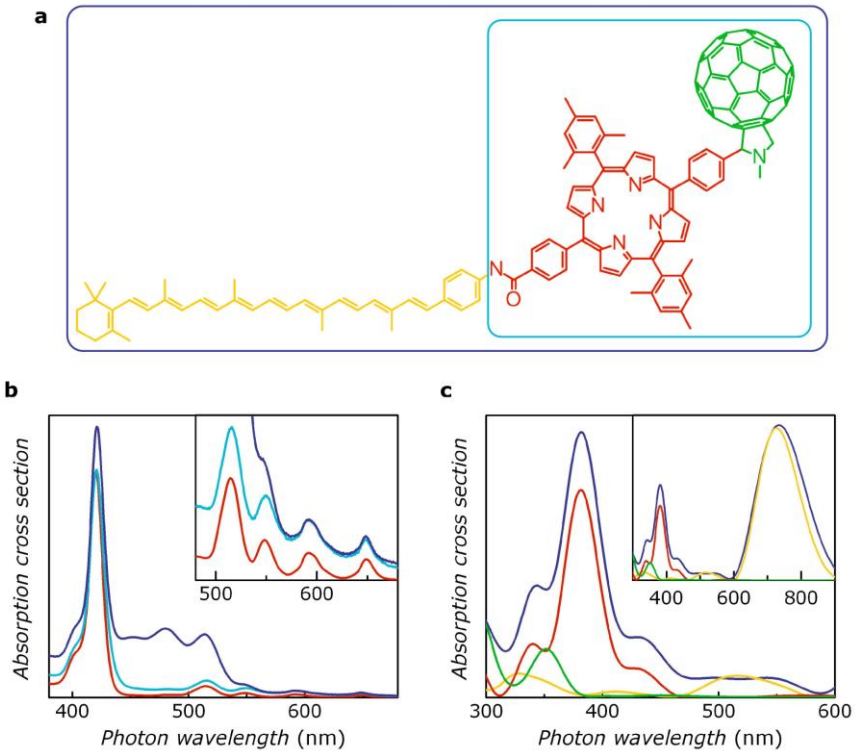

Figure 1: Experimental and theoretical absorption spectroscopy. (a) Chemical structure of the carotene-porphyrin-fullerene light-harvesting triad. **(b)** Measured normalized absorption spectra of the triad (dark blue), a porphyrin-fullerene dyad (light blue) and an individual porphyrin-unit (red) in toluene solution. The spectra have been normalized to the height of the low-energy porphyrin peaks which are depicted magnified in the inset. **(c)** Absorption spectra of the triad and their individual subunits simulated by time-dependent density functional theory. The triad absorption is well represented by a sum of the different subunit spectra, in accord with experiment. The porphyrin bands match reasonably well with the observed ones, once a rigid red-shift of 180 meV is applied to the computed

spectrum. The red-shift of the main carotene peak to 730 nm reflects the excitonic quantum confinement in the quasi-one-dimensional carotene chain[21].

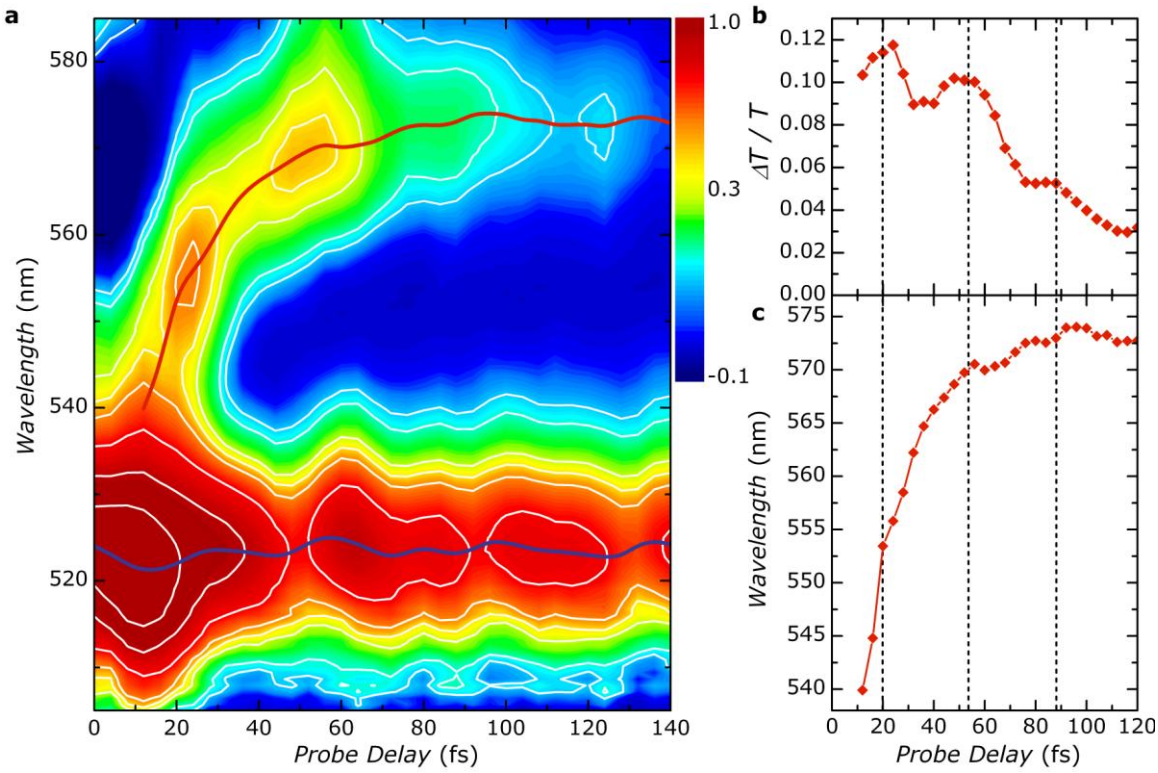

Figure 2: Coherent charge transfer dynamics in a carotene-porphyrin-fullerene triad. (a) Experimental differential transmission ($\Delta T / T$) map as a function of time delay and probe wavelength recorded following impulsive excitation of the triad at around 550 nm. The blue and red lines highlight the time evolution of the center wavelengths of the porphyrin and charge transfer bands, respectively. These center wavelengths have been extracted from the experimental data by fitting the $\Delta T / T$ spectra of both bands to Gaussian lineshape functions. **(b,c)** Temporal evolution of the $\Delta T / T$ amplitude (b) and spectral position (c) of the charge transfer band. The dashed lines are guides to the eye, emphasizing coherent oscillations of both amplitude and center

wavelength of the charge transfer resonance.

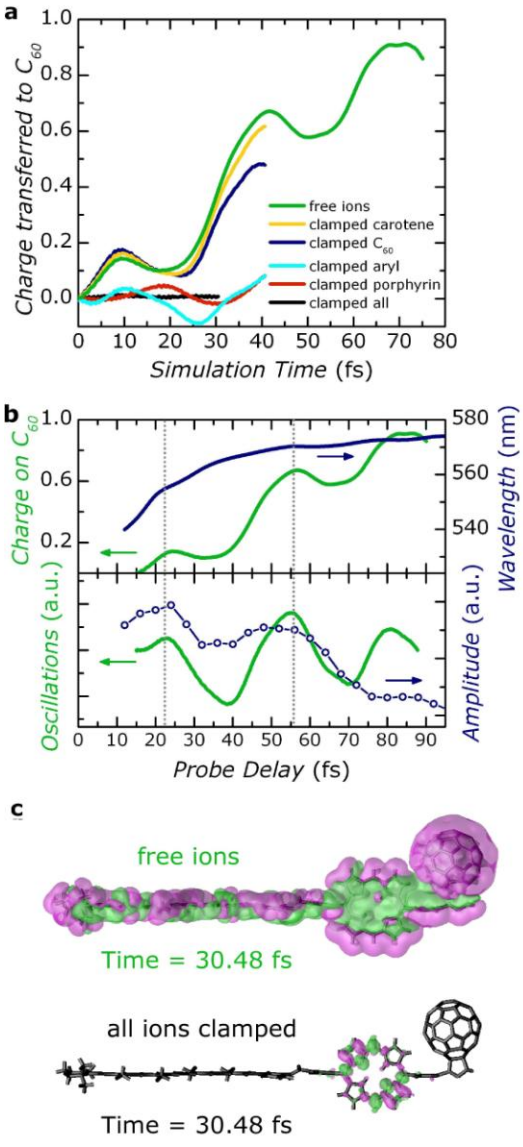

Figure 3. **Quantum dynamics simulations of the charge transfer process. (a)** Simulated charge transfer in the triad occurs in about 70 fs (green line). Temporal oscillations with a period of about 30 fs suggest that coherent nuclear motion drives this charge transfer. The dynamics remain unaltered when locking the positions of either the carotene (yellow line) or the fullerene (blue). Clamping the porphyrin (red), or only 4 atoms (cyan) on the connector between porphyrin and fullerene fully suppresses the charge accumulation. **(b)** Correlation between temporal oscillations in the simulated transferred charge (green lines, in lower panel the slow exponential rise was subtracted, and a time shift of 15 fs was applied) and in the resonance wavelength (blue, upper panel) and the amplitude (blue, lower panel) of the differential transmission spectrum of the charge

transfer band. This correlation is evidence for the coherent motion of electrons and nuclei during the charge transfer. **(c)** Snapshots of the photoinduced change in charge density at a time delay of 30.48 fs for the free triad (upper panel) and with all atoms clamped. Magenta indicates an increase in electronic charge density, whereas a decrease is shown in green.

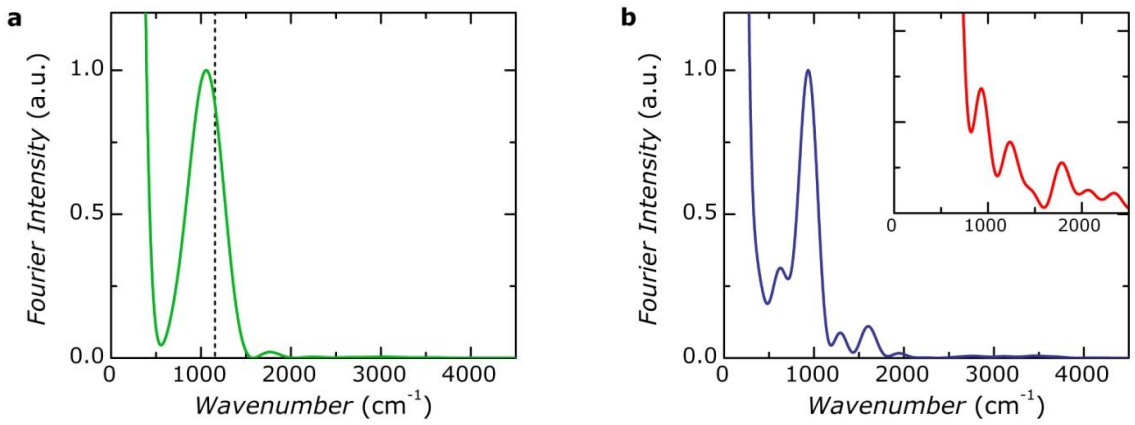

Figure 4: Fourier intensity spectra of the charge transfer dynamics in a carotene-porphyrin-fullerene triad. Fourier intensity spectrum of the simulated charge transfer dynamics towards the fullerene (**a**, data taken from Fig. 3a), showing a resonance at 1060 ± 190 cm^{-1}, and of the temporal variation of the (ΔT/T) amplitude of the charge transfer band (**b**, data taken from Fig. 2b) with a resonance at 940 ± 100 cm^{-1}, corresponding to an oscillation period of 35 fs. The inset in panel (**b**) displays the Fourier intensity spectrum of the observed temporal red-shift of the charge transfer band (data taken from Fig. 2c), revealing a dominant peak at 930 ± 90 cm^{-1}. The broad shoulder below 820 cm^{-1} reflects the pronounced shift in resonance wavelength in Fig. 2c on a 100-fs-timescale. The black dashed line indicates the frequency of the carotene symmetric C-C stretch mode at 1155 cm^{-1}. The data were padded to zero with exponentially decaying tails at both sides before Fourier transformation. We take the fact that the main oscillatory resonance in the Fourier transforms of both the time-dependent amplitude and resonance wavelength peaks around 940 cm^{-1} as experimental signature that the differential transmission spectra of the charge transfer band are modulated by an

oscillatory wavepacket motion with a period of about 30 fs. Within our signal-to-noise ratio this matches well with the oscillation period seen in the simulated charge transfer dynamics, reflecting the nuclear motion of the carbon backbone.